N89-24712

Modelling and Design of High Performance Indium Phosphide Solar Cells

Sandra L. Rhoads
AstroPower Division/Astrosystems, Inc.

Allen M. Barnett
University of Delaware

Abstract

A first principles pn junction device model has predicted new designs for high voltage, high efficiency InP solar cells. Measured InP material properties were applied and device parameters (thicknesses and doping) were adjusted to obtain optimal performance designs. Results indicate that p/n InP designs will provide higher voltages and higher energy conversion efficiencies than n/p structures. Improvements to n/p structures for increased efficiency are predicted. These new designs exploit the high absorption capabilities, relatively long diffusion lengths, and modest surface recombination velocities characteristic of InP.

Predictions of performance indicate achievable open-circuit voltage values as high as 943 mV for InP and a practical maximum AM0 efficiency of 22.5% at 1 sun and 27°C. The details of the model, the optimal InP structure and the effect of individual parameter variations on device performance will be presented.

Introduction

The goal of this study was to derive InP solar cell designs yielding high open-circuit voltage without significantly sacrificing short-circuit current. It is appropriate to begin such a study with a look at today's InP solar cell designs. The widely accepted optimum design for InP solar cells is an n+/p/p+ structure offering a maximum open-circuit voltage of 902 mV for epitaxial structures [ref. 1]. However, from first principles, open-circuit voltages well above 900 mV should be achievable for a bandgap of 1.35 eV. The design requirements yielding maximum voltage and maximum energy conversion efficiency for InP solar cells are described.

The highest efficiency InP solar cells were reported by Keavney and Spitzer [ref. 2]. The device structure was an n+/p/p+ design formed by silicon ion implantation of epitaxial material. Wanlass et. al. [ref. 3] has also reported high efficiency InP solar cells fabricated using MOCVD. The device parameters and experimental results are shown in Table 1 and Table 2. These tables also include the device parameters and predicted performance of the near-optimum structure predicted by Goradia

[ref. 1]. It is important to note that all three designs are very similar. All have an ultrathin emitter layer, an emitter with a high carrier concentration and a base with a low carrier concentration.

Theoretical Model

The model used in this study is based on the diode equation. Reverse saturation current and short-circuit current are expressed as basic solutions to transport equations derived by many different authors [refs. 4,5] for the pn junction. This study uses standard modelling assumptions of one-dimensional carrier movement, low-level injection and uniform doping. It calculates the reverse saturation current contributed by the emitter and the base, and the short circuit current contributed by the emitter, base, and depletion region. These current equations describe the minority carrier behavior in each region of a solar cell structure.

The expression for open-circuit voltage is of standard form – – proportional to the natural log of the ratio of short-circuit current and reverse saturation current. The expression used for fill factor is based on the ideal definition which expresses fill factor as a function of open-circuit voltage only [ref. 6].

The reverse saturation current and short-circuit current values predicted by the equations described above include loss mechanisms inherent to InP according to its material properties. These current values are sensitive to surface recombination velocities, diffusion lengths, and minority carrier lifetimes which reflect material purity and quality.

Additional corrections were made to short-circuit current and fill factor values to account for device losses. Short-circuit current values were reduced by 6.6% for grid shading and reflection losses. Fill factor values were reduced by 2% to account for series resistance losses. These specific percentages were determined for GaAs [ref. 7], however, electrical losses for InP solar cells are expected to be the same.

For calculation of light generated current, detailed knowledge of the solar spectrum is required. The solar spectrum was divided into narrow bands such that photon flux and absorption coefficient could be considered constant within each band. The current generated within each band was calculated and then all band currents were summed together to yield the current generated over the entire usable solar spectrum.

Flux, as a function of wavelength, was obtained from the solar spectral-irradiance standard curve (AM0) [ref. 8] generated by measurements from aircraft. The total amount of power incident from the sun at unit area in the orbit was determined to be 135.3 mW/cm^2. Optical constants for determination of absorption coefficient as a function of wavelength were obtained from the Handbook of Optical Constants [ref. 9].

Values for minority carrier diffusion length as a function of carrier concentration were taken from experimental results published by Yamaguchi et al [ref. 10]. The data were determined from the relationship between photoluminescence intensity and carrier concentration in InP and that between solar cell photoresponse and carrier concentration in InP. Values for mobility as a function of carrier concentration were taken from experimental results published by Kuphal [ref. 11] for liquid phase epitaxial InP. Characterization was performed mainly by Van der Pauw and capacitance-voltage (C–V) measurements.

The results predicted by the device modelling studies are sensitive to the material parameters (intrinsic carrier concentration, mobilities, diffusion lengths, lifetimes) assumed by the model. Great care was taken in this study to use conservative values; the material parameter data used in this study are more conservative than estimates used by others. The material parameters assumed for the optimum device designs predicted by this model are listed in Table 3.

Baseline Study

As a baseline test of this model, the device parameters used for the experimental devices by Wanlass et al were introduced to our model using the material parameter data (such as mobility and diffusion length as a function of carrier concentration) discussed above.

Figure 1 is a plot of the resulting open-circuit voltage and conversion efficiency values predicted for a wide range of emitter carrier concentrations. The conversion efficiencies predicted by Goradia and achieved by Spire [ref. 2] and SERI [ref. 3] have been added for comparison. Note that Goradia's model and this model are in complete agreement for the given n+/p/p+ design. The experimental results indicate that the n+/p/p+ design described by Goradia is being successfully fabricated.

Table 1 indicates that a major difference exists between Goradia's model and this model in the material parameters of the p-type base. Mobility values are similar, however diffusion length and minority carriers lifetime values are extremely different for the same carrier concentration. Differences in performance are reflected in the predicted open-circuit voltage values shown in Table 2. Goradia predicts lower reverse saturation currents are achievable – – open-circuit voltage is higher.

InP Design Optimization Results

Figure 1 indicates an upward trend in efficiency as emitter doping is lowered. By lowering the emitter doping and raising the base doping, the conversion efficiency predicted for the n/p design can be increased as shown in Figure 2.

A further increase in efficiency can be realized if the emitter layer is expanded to 0.29 microns. In fact, as shown in Figure 3, efficiency actually increases with increasing emitter thickness up to 0.29 microns. Figure 3 also illustrates that for the n/p+ design, efficiency is not extremely sensitive to wide variations in emitter thickness. The maximum efficiency for this design is 21.5%, corresponding to a 7% gain in efficiency over the traditional n+/p/p+ structure. This design maximizes current gain in the emitter while open-circuit voltage remains relatively constant. Table 3 provides device parameters for this optimized design.

The maximum attainable voltage and efficiency for an InP solar cell is predicted for a p/n design. A 943 mV maximum is predicted for a 2×10^{18} base and emitter, however this is not a maximum efficiency design. A design with a more traditional emitter to base doping ratio offers the maximum efficiency of 22.5%. This design is sensitive to emitter thickness and requires an emitter less than or equal to 0.07 microns. The details of the optimized p/n structure are given in Table 3.

A careful comparison of n/p and p/n InP designs suggests a physical dependence of the InP solar cell on the properties of its p-type layer which determines the optimum device parameters. Table

3 reveals that the optimal p-type carrier concentration in both designs is identical – – 6×10^{16}. The p-type material, whether it forms the emitter or the base, is the main contributor to reverse saturation current. For n/p designs, the only way to significantly reduce (by an order of magnitude) reverse saturation current is to increase base doping; this explains the n/p+ design being optimum rather than an n+/p design. As shown in Figure 5, variations in emitter doping have no effect on total J_0 for n/p designs.

For p/n designs, J_0 is still dominated by the p-type component. However, by increasing emitter doping (Figure 6) and decreasing base doping, saturation current can be brought to an absolute minimum. This explains why the p+/n is the absolute optimum device design for a high voltage, high efficiency InP solar cell.

Another comparison of n/p and p/n designs is presented in Figures 7 and 8. Short-circuit current and open-circuit voltage values remain relatively unchanged within a certain range of surface recombination velocity values. For the n/p structure, the surface recombination limit is about 1×10^3. For the p/n structure, the limit is about 1×10^5. These values are in agreement with the physical constants listed for InP by Coutts [ref. 12].

Figures 7 and 8 also uncover another difference between n/p and p/n InP designs. The reduction in short-circuit current is less drastic for the p/n design as surface recombination exceeds its acceptable limit. Absorption in the n/p design occurs primarily in the emitter; an increase in surface recombination velocity drastically reduces the number of collectable carriers. The short-circuit current of the p/n design is less emitter-dependent. Significant absorption takes place within the depletion region and base layer where minority carrier diffusion lengths are longer; a larger number of carriers are collected beyond the emitter layer.

Conclusions

The significance of this model is three fold. This model:

(1) provides nontraditional designs for high voltage, high efficiency InP solar cells.

(2) reveals that the p-type material (through reverse saturation current) is the key to high voltage, high efficiency InP solar cell performance.

(3) supports the conversion efficiency predicted for the traditional n+/p/p+ InP solar cell.

Acknowledgement

Special thanks is extended to Dr. Timothy J. Coutts for helpful discussions and for a copy of his InP review paper [ref. 12].

References

[1] C. Goradia, J. V. Geier, and I. Weinberg, "Modelling and Design of High Efficiency Radiation Tolerant Indium Phosphide Space Solar Cells", *Proceedings of the 19th IEEE PVSC*, New Orleans, Louisiana, (1987), p. 937.

[2] C.J. Keavney and M.B. Spitzer, "Indium Phosphide Solar Cells Made by Ion Implantation", Appl. Phys. Lett. **52** (17), (1988), p. 1439.

[3] M.W. Wanlass, T.A. Gessert, K.A. Emery, and T.J. Coutts, "Empirical and Theoretical Studies of the Performance of OMCVD InP Homojunction Solar Cells as a Function of Emitter Thickness and Doping, and Base Doping", presented at this conference.

[4] C. Hu and R.M. White, "Solar Cells: From Basic to Advanced Systems", McGraw-Hill, Inc., (1983), p. 51)55.

[5] H.J. Hovel, *Semiconductors and Semimetals, vol. 2 (Solar Cells)*, ed. Willardson and Beer, Academic Press, Inc., (1975), p.18.

[6] M.A. Green, *Solar Cells*, Prentice-Hall, Inc., (1986), p. 80.

[7] J. B, McNeely, G. H. Negley, M. E. Nell, S. F. Brennan, A. M. Barnett, "Design and Fabrication of GaAsP Top Solar Cells", *Proc. 18th IEEE PVSC*, (1985), p. 151.

[8] M.P. Thekaekara, "Extraterrestrial Solar Spectrum, 3000-6100 Åat 1-ÅIntervals", Applied Optics **13**, No. 3, (1974), p.518.

[9] O.J. Glembocki and H. Pillar, in *Handbook of Optical Constants of Solids*, ed. E.D. Palik, Academic Press, Inc., New York (1985), p. 503.

[10] M. Yamaguchi, A. Yamamoto, N. Uchida and C. Uemura, "A New Approach for Thin Film InP Solar Cells", Solar Cells, **19** (1986-1987) p. 85.

[11] E. Kuphal, "Preparation and Characterization of LPE InP", Journal of Crystal Growth, **54**, 117 (1981).

[12] T.J. Coutts and M. Yamaguchi, "InP Based Solar Cells: A Critical Review of Their Fabrication, Performance and Operation", Current Topics in Photovoltaics, **3**, Academic Press, London, to be published, 1988.

TABLE 1: **Device parameters of the accepted n+/p/p+ optimum design.**

	Goradia's Model	SPIRE Device	SERI Device	This * Model
emitter:				
thickness (μm)	.04	.03	.025	.025
doping ($1/cm^3$)	6×10^{17}	3×10^{19}	4×10^{18}	4×10^{18}
diffusion length (μm)	1.00	------	------	0.36
mobility (cm/V-s)	93.4	------	------	66.0
lifetime (ns)	4.19	------	------	0.76
base:				
thickness (μm)	1.5	3.0	3.0	3.0
doping ($1/cm^3$)	5×10^{16}	2×10^{16}	5×10^{16}	5×10^{16}
diffusion length (μm)	12.8	------	------	2.3
mobility (cm/V-s)	3550	------	------	3566
lifetime (ns)	17.9	------	------	.57

*Intrinsic carrier concentration (n_i^2) = 1.5×10^{14}

TABLE 2: **Performance parameters for the accepted n+/p/p+ optimum design.**

	Goradia's Model	SPIRE Device	SERI Device	This Model
Voc (mV)	901.6	873	882	883
Jsc (mA/cm^2)	36.53	35.7	33.06	36.2
FF (%)	84.79	82.9	82.6	85.3
AM0 Eff. (%)	**20.34**	**18.8**	**17.6**	**20.1**

Table 3: **New high voltage, high efficiency designs predicted by this model.**

	N/P	P/N
emitter:		
thickness (μm)	.22 to .56	.02 to .07
doping ($1/cm^3$)	2×10^{16}	6×10^{17}
diffusion length (μm)	3.0	.80
mobility (cm/V-s)	145.0	2292.0
lifetime (ns)	24.0	.11
base:		
thickness (μm)	5.0	5.0
doping ($1/cm^3$)	6×10^{17}	6×10^{16}
diffusion length (μm)	.80	2.7
mobility (cm/V-s)	2292.0	130.0
lifetime (ns)	.11	22.0
front surface rec. (cm/s)	1×10^3	1×10^5
back surface rec. (cm/s)	1×10^7	1×10^7

Table 4: **Predicted performance for the new designs described in Table 3.**

	N/P	P/N
Voc (mV)	901	928
Jsc (mA/cm^2)	37.7	38.2
FF (%)	85.5	85.8
Efficiency (AM0)	**21.5%**	**22.5%**

Figure 1: **Open-circuit voltage and efficiency predictions of this model assuming SERI's emitter thickness, base doping, and base thickness.**

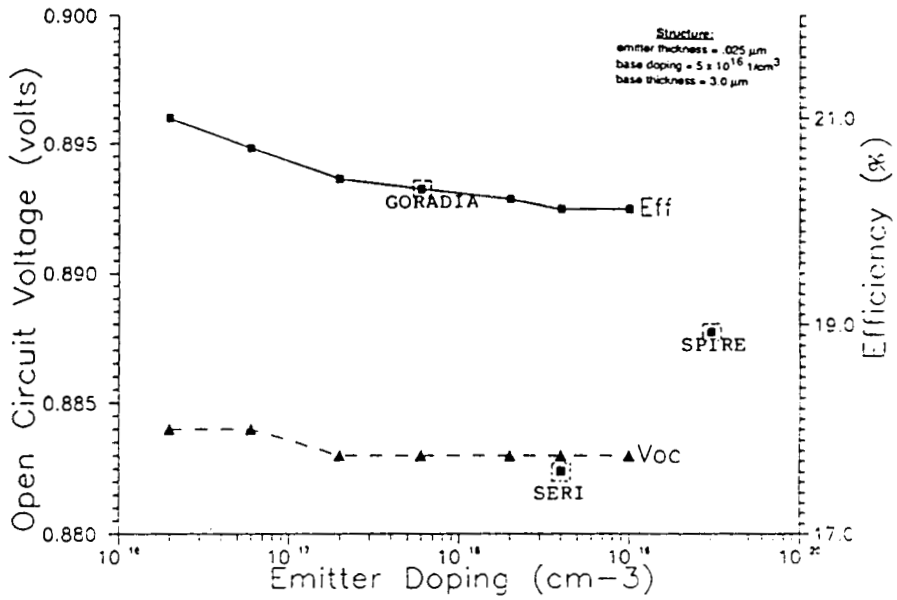

Figure 2: **Higher efficiency is predicted for the N/P structure if the emitter concentration is reduced and the base concentration is increased.**

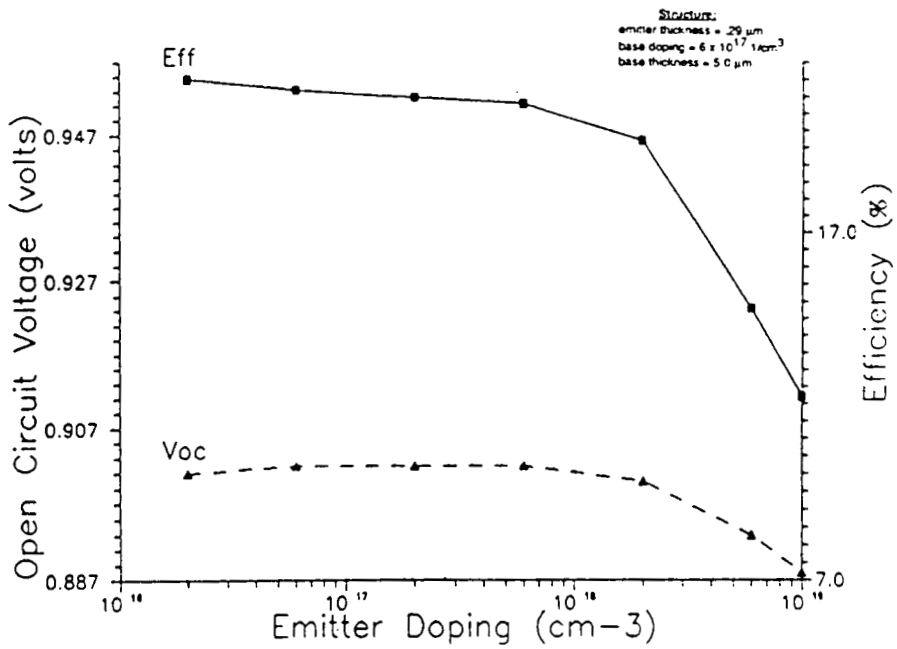

C-2

Figure 3: **The N/P+ design offers a wide range of acceptable emitter thicknesses yielding high efficiencies.**

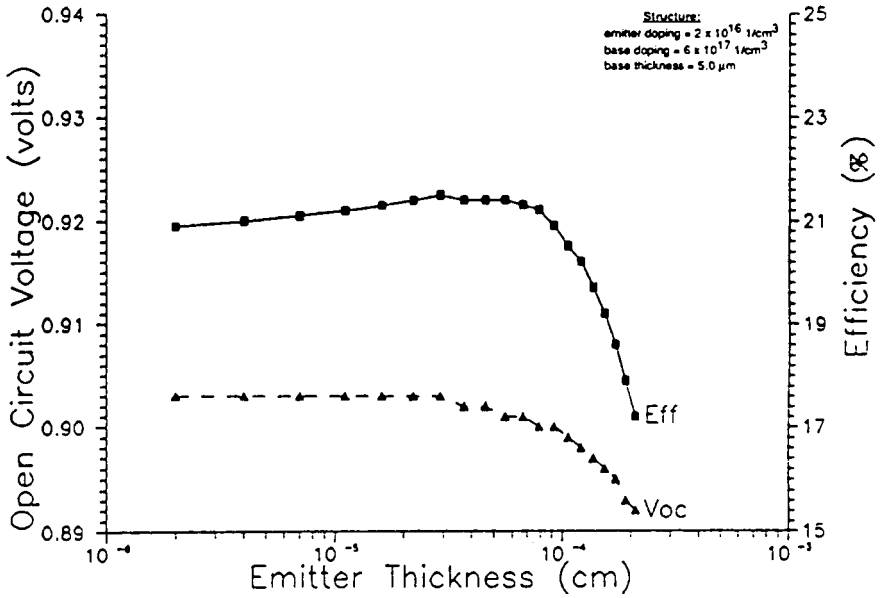

Figure 4: **The highest efficiency design predicted by this model is a P/N structure.**

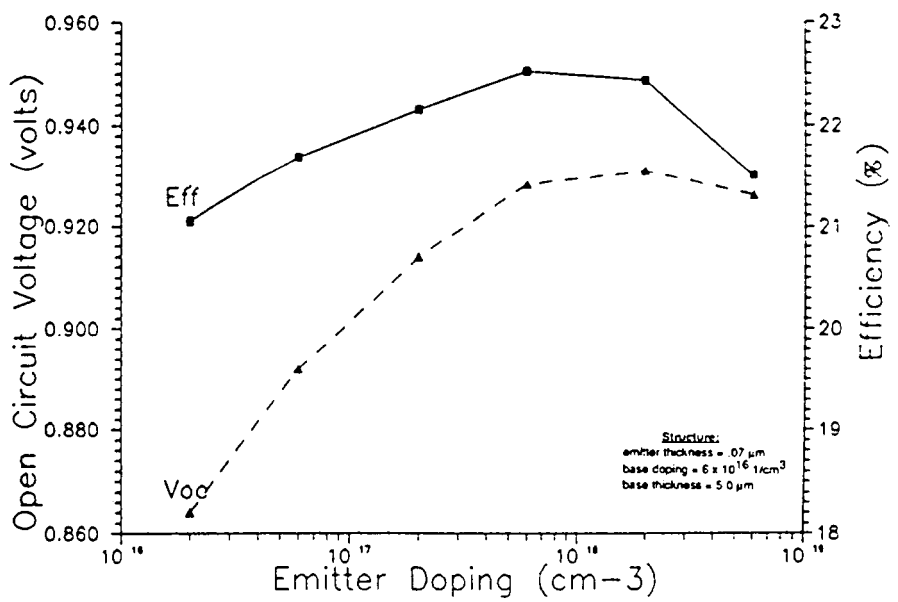

Figure 5: **Jo of the optimum N/P+ design (Figure 2) is dominated by its base (P-type) component.**

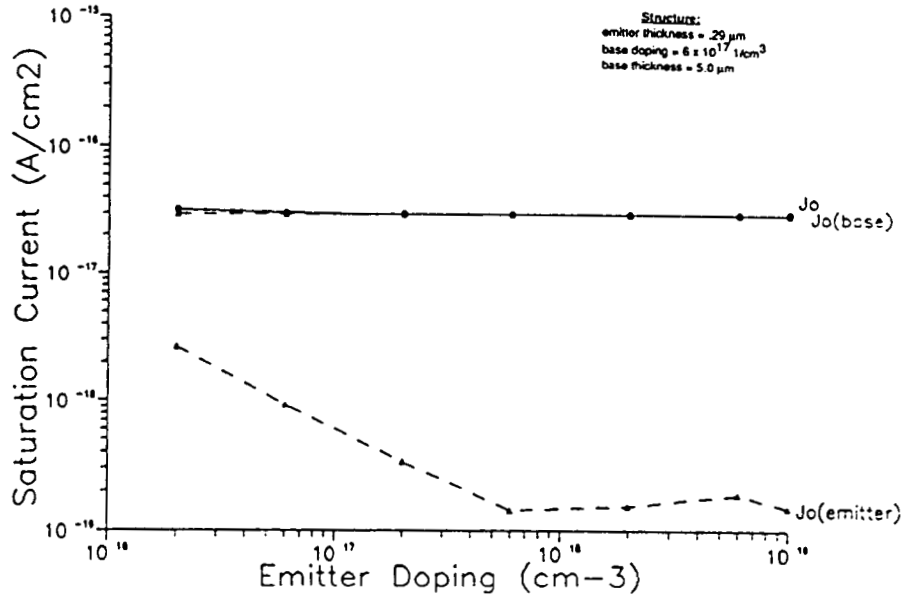

Figure 6: **Jo of the optimum P/N design (Figure 4) is dominated by its emitter (P-type) component.**

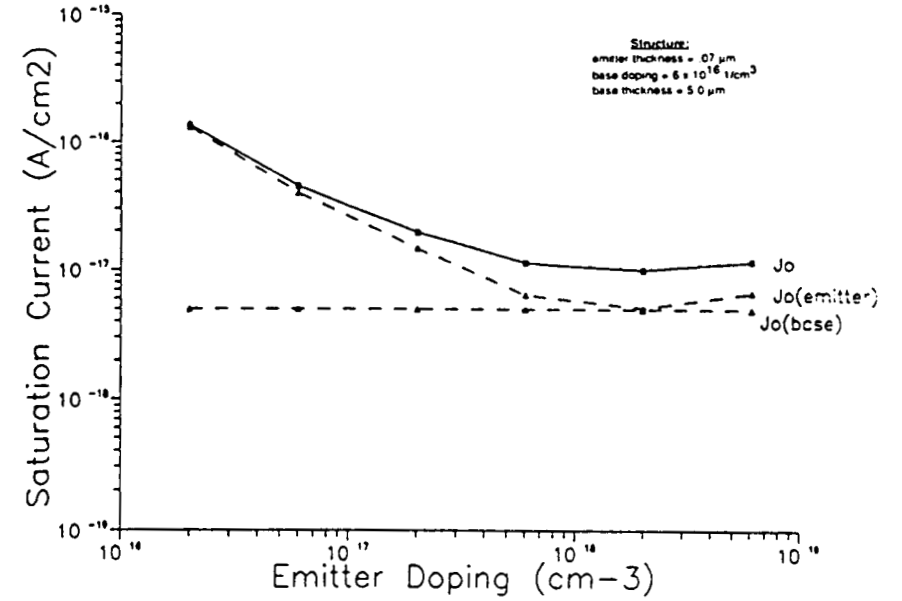

Figure 7: **Acceptable bounds for front surface recombination velocity for the optimum N/P+ design.**

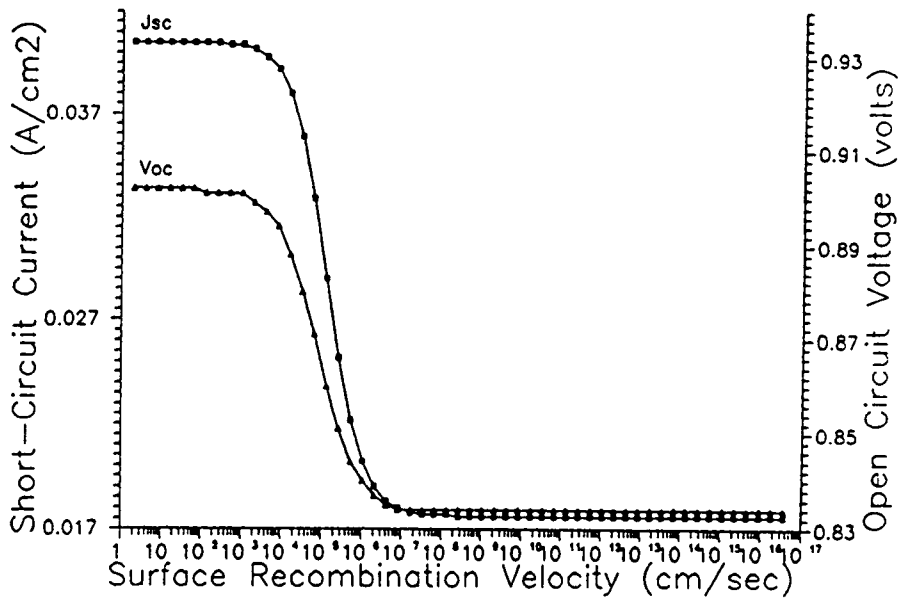

Figure 8: **Acceptable bounds for front surface recombination velocity for the optimum P/N design.**